J Nondestruct Eval (2013) 32:372–383
DOI 10.1007/s10921-013-0191-y

Experimental Study on Ultrasonic Monitoring of Splitting Failure in Reinforced Concrete

Magdalena Rucka · Krzysztof Wilde

Received: 6 February 2013 / Accepted: 5 July 2013 / Published online: 24 July 2013
© The Author(s) 2013. This article is published with open access at Springerlink.com

Abstract This paper investigates inspection of reinforced concrete elements sensitive to the splitting failure. The behaviour of a reinforced concrete specimen subjected to a tensile stress is considered. The damage detection procedure is based on the ultrasonic wave propagation technique. The piezoelectric transducers are located on both ends of the specimen and the measurements are taken periodically during the incrementally increased loading. The features of measured signals in time and frequency domains as well as wavelet transforms before and after the splitting failure are studied. The experimental results show that proposed method can be used for monitoring of damage evolution in concrete elements. The method makes possible detection of the moment just before the splitting failure occurs.

Keywords Ultrasonic testing · Wave propagation · Reinforced concrete · Splitting failure · Damage evolution

1 Introduction

Reinforced concrete is a material commonly and widely used for building structures. Concrete in structures like bridges, dams, silos, towers or tall buildings is continuously degraded due to static and dynamic loading, corrosive factors, changes in temperature and humidity. Continuous environmental and operational loadings cause concrete cracking within the range that is considered in the design process. Small, permissible cracks do not affect the concrete element durability. However, for some concrete elements cracking can result in the splitting failure. In such case the crack opening is relatively large and splitting of the concrete cover exposes the reinforcing bars. Therefore, detection of damage at an early stage of degradation is of great interest to the civil engineering community.

In recent years, various damage detection techniques incorporated in structural health monitoring systems have been investigated to improve the safety of structures and to extend the structure service life. Many methods have been developed for nondestructive evaluation, e.g. acoustic emission [1, 2], infrared thermography [3] or ultrasonic testing [4–7]. Of particular interest are impact-echo techniques [8, 9] and methods based on propagation of elastic waves [10, 11]. In general, two approaches have been applied to register propagating waves. The first approach is directed towards non-contact techniques, based on speckle interferometry (e.g. [12]) or laser vibrometry (e.g. [13–15]). Another approach depends on using transducers on the specimen surface (e.g. [16]). The conventional ultrasonic transducers are rather bulky and expensive, thus recently piezoelectric ceramic transducers (PZT) have been commonly used, since they are small, lightweight, unobtrusive and inexpensive, and can be produced in different geometries [17]. The ultrasonic or PZT transducers can act as both actuators (transmitting transducers) and sensors (receiving transducers), and if a receiving transducer is bonded at a remote point of a structure, the received signal contains information about the integrity of the line between them [16]. A wide range of studies has already been reported on the application of ultrasonic waves to evaluate structure condition before and after damage, in particular wave scattering from damage in the form of artificially cut notch, crack or slot,

M. Rucka (✉) · K. Wilde
Department of Structural Mechanics and Bridge Structures, Faculty of Civil and Environmental Engineering, Gdansk University of Technology, ul. Narutowicza 11/12, 80-233 Gdańsk, Poland
e-mail: mrucka@pg.gda.pl

K. Wilde
e-mail: wild@pg.gda.pl

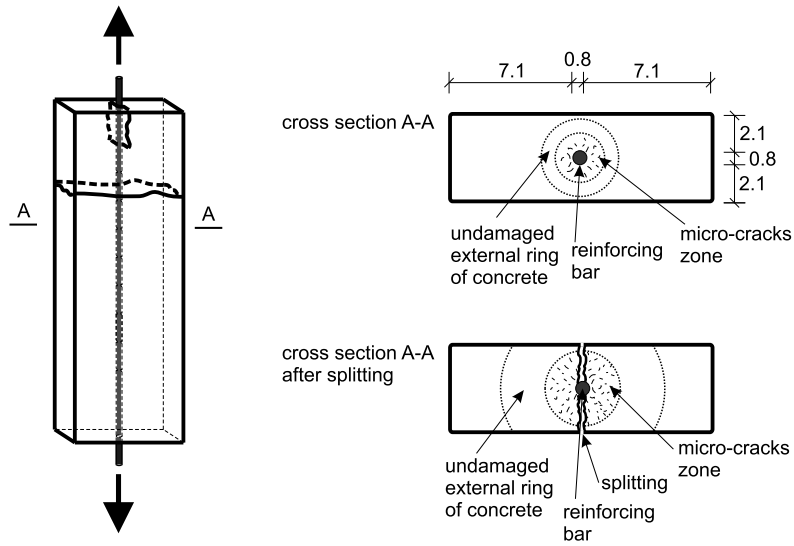

Fig. 1 Considered concrete specimen in tension and sketch of formation of micro-cracks before and after splitting (dimensions shown in cm)

e.g. [10, 13, 15, 16]. There are also applications of wave propagation methods for fatigue crack detection in metallic structures, e.g. [14]. Novelty of this paper is a systematic study on ultrasonic wave propagation in the forms of wave packets for monitoring of the splitting failure in reinforced concrete elements under incrementally increased loading.

The splitting failure is a complex phenomenon that can lead to a collapse of a whole concrete element. Sensitive to the splitting failure are elements with reinforcement bars in tension with high bound stresses like anchorages with limited transverse pressure, heads of pre-stressed, pre-tensioned thin webbed beams [18]. The splitting failure of concrete elements is caused by a local collapse of the bond between steel bars and surrounding concrete. During loading, at first stage, radial micro-cracks develop in a limited zone around the reinforcement bar. The external ring of undamaged concrete provides sufficient confinement that prevents splitting. At large external loads the undamaged external ring becomes too thin and cracks spread through the element. When the splitting failure occurs the bond between the reinforcement and concrete is lost and cracks are wide open resulting in significant reduction of loading capacity. Problems of the bond and the splitting failure have been investigated by many researchers, e.g. [18–20]. Gambarova et al. [18] carried out tests on the concrete splitting along an anchored bar subjected to a pull-out force. Numerical analyses of the bond splitting failure were conducted by Ogura et al. [19]. Gálvez et al. [20] presented an experimental study on the bond-splitting in precast prestressed concrete during the release of a prestressing force. They examined the longitudinal splitting of the concrete specimens of dimensions 40 × 6 × 6 cm with one wire of diameter 4 mm embedded longitudinally in the specimen. The release of the load in the wire caused the longitudinal splitting of the concrete prism.

This paper focuses on monitoring of concrete elements subjected to tensile loading resulting in the splitting failure. The monitoring is conducted with use of ultrasonic waves generated and measured by the PZT transducers. The proposed procedure assumes semi-continuous ultrasonic testing during the element full loading cycle. The PZT transducers are installed on both ends of the concrete specimen. Analyses of time and frequency characteristics of the ultrasonic signals propagating through the whole element are used to detect concrete cracking and for evaluation of element condition. In this paper, the experimental splitting failure of reinforced concrete is ensured by selection of a concrete specimen with the rectangular cross-section in which one dimension is three times larger than the other. Therefore, formation of micro-cracks [18] at low level of external loading is limited to a zone surrounded by the undamaged concrete ring (Fig. 1). At large loadings the micro-crack zone increases and finally the splitting failure takes place. The aim of the paper is an experimental verification of detection possibility of concrete micro-cracking before the splitting failure occurs by means of ultrasonic monitoring and frequency and wavelet analysis.

2 Experimental Setup

2.1 Description of Specimen

The concrete specimen with cross-section of 5 cm × 15 cm and length of 70 cm was considered as the testing element. Figure 2 presents the geometry and dimensions of the tested specimen. The ingredients of concrete were: Portland cement type CEM I 42.5R, sand (0–2 mm), fine aggregate (2–8 mm), coarse aggregate (8–16 mm), ash and superplasticizers. The proportion of concrete mix is outlined in Ta-

MOST WIEDZY Downloaded from mostwiedzy.pl

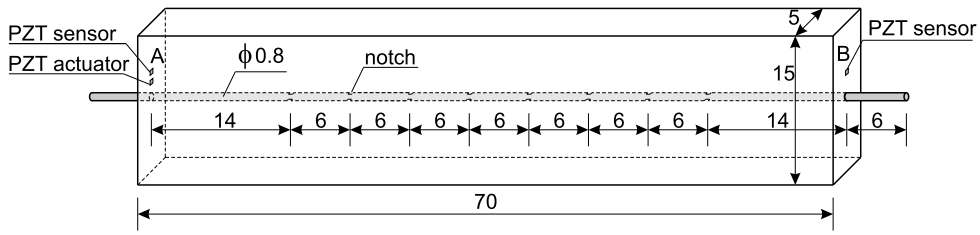

Fig. 2 Geometry and dimensions of the tested reinforced specimen (dimensions shown in cm)

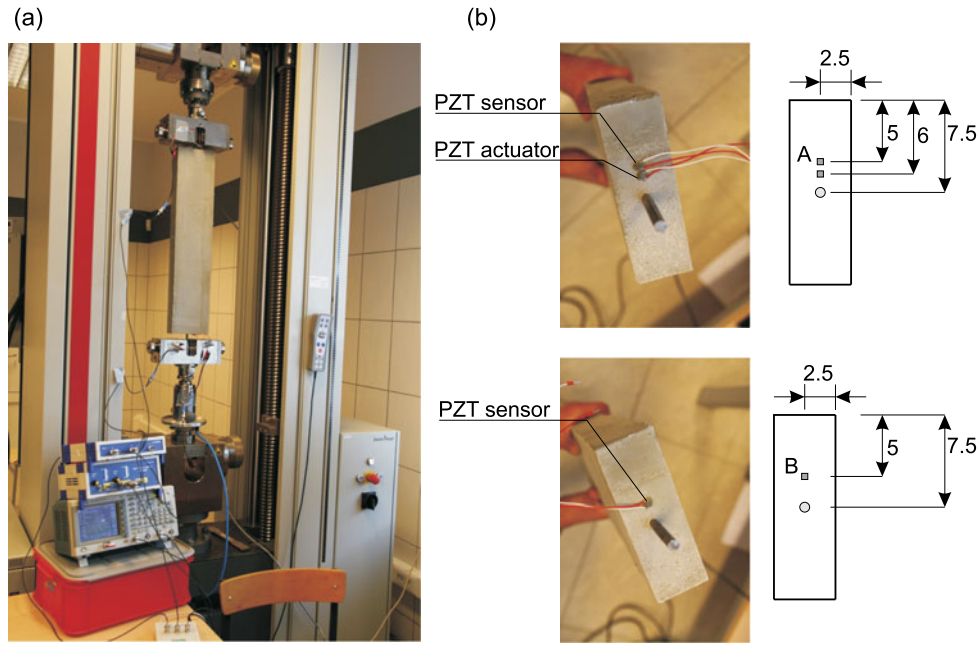

Fig. 3 Experimental set-up for measurements of ultrasonic waves in the reinforced specimen under tensile loading: (**a**) photograph of instrumentation; (**b**) details showing location of PZT actuator and PZT sensors on the specimen (dimensions shown in cm)

Table 1 Mixture proportion of concrete

Material	Water	Cement	Sand	Aggregates	w/c ratio	Ash	Superplasticizers
kg/m^3	180	240	819	940	0.75	85	3.41

ble 1. The specimen was reinforced in longitudinal direction with one deformed steel bar of diameter 8 mm. Eight notches were cut on the bar at the distance of 6 cm (Fig. 2). The notches were applied to ensure that the splitting failure occurred within the concrete part of the specimen and to avoid damage of the bar outside of the concrete prism. The large number of notches was cut to cause relatively homogeneous damage zone that can be easily detected by ultrasonic methods.

2.2 Tensile Process Testing

The concrete specimen was subjected to axial tensile loading applied at both exposed ends of the embedded bar. The tensile tests were carried out in a testing machine Zwick/Roell Z400 using displacement control with the speed of the crosshead of 0.5 mm/min. The photo of the experimental set-up is shown in Fig. 3a.

2.3 Ultrasonic Testing

During the tensile test, ultrasonic elastic waves were generated and propagated through the specimen. The ultrasonic waves were excited in the longitudinal direction by means of a plate PZT actuator Noliac CMAP11 of dimensions 5 mm × 5 mm × 2 mm bonded at the end of the concrete specimen by wax. Two PZT sensors bonded on both ends of the concrete specimen (sensors A and B, as depicted in Fig. 2 and Fig. 3b) were utilized for wave sensing. An arbitrary waveform generator (Tektronix AFG 3022) with a high voltage amplifier (EC Electronics PPA 2000) created an excitation voltage signal applied next to the PZT actuator, which converted it into a mechanical force. As a result of application the voltage amplifier the measured signal was amplified ten times. A digital oscilloscope (ScopeDAQ) was used to collect the A-scan signals with a sampling frequency of 1 MHz. During the tensile test, the ultrasonic wave signals were excited and acquired every 15 s, until the speci-

MOST WIEDZY Downloaded from mostwiedzy.pl

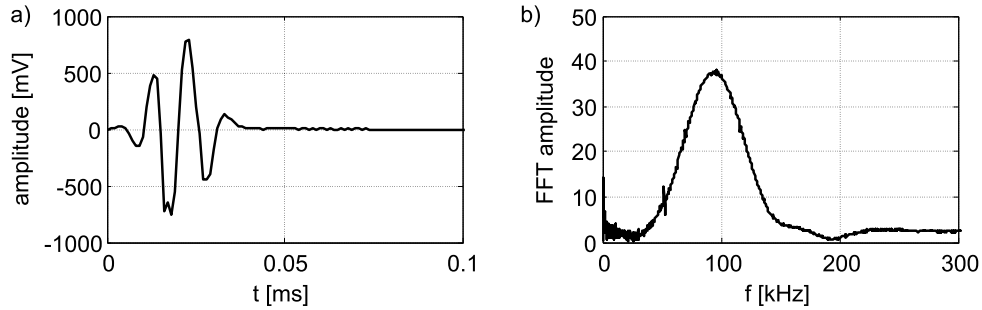

Fig. 4 Excitation signal: (**a**) in time domain; (**b**) in frequency domain

men failure. The ultrasonic tests were carried out on three the same concrete specimens with centrally embedded bar.

The excitation signal considered in this study was chosen as a single-frequency smoothed tone burst (also known as a wave packet) obtained from the multiplication of a sinusoidal function of established frequency by a Hanning function. The Hanning window provides smoothed tone burst in order to reduce the excitation of side frequencies [17]. This aspect of excitation of coherent single-frequency waves is important in the context of ultrasonic diagnostics. The number of cycles in the tone burst has a strong influence on the bandwidth of the input signal. For the established frequency of the sine wave, a large number of cycles is advantageous to obtain a narrow band in the frequency domain. On the other side, too many cycles causes increasing of wave packet length in the time domain. In this study, a four-peak sinusoidal signal with a central frequency of 96 kHz modulated by the Hanning window (Fig. 4) was chosen as a compromise between acceptable level of resolution in the time and frequency domains.

3 Test Results and Discussion

3.1 Mechanical testing results

During the tensile tests, the displacement of the cross-head and the force level were recorded. Figure 5 shows the force-displacement (P–u) and the force-time (P–t) curves for the tested specimens. There are sudden drops of the force at the moments when the major splitting cracks appear and the load distribution within the specimen alters in time. It was noted that the sizes of the notches were not identical within the given element since they were cut by hand. The time of duration of the tensile test was 1770 s, 1590 s and 1710 s for specimen no. 1, no. 2 and no. 3, respectively. The maximum displacement $u_{\max}$ of the cross-head in the longitudinal direction was 7.38 mm, 6.6 mm and 7.12 mm for specimen no. 1, no. 2 and no. 3, respectively. During the tensile test, wave propagation measurements were conducted. Time signals were taken each 15 seconds and each signal was assigned ordinal number n. Parameter n started from $n = 1$ and reached $n = 119$ for specimen no. 1, $n = 107$ for specimen no. 2 and $n = 115$ for specimen no. 3. Additionally, photographs were taken to observe the damage evolution at the front side of the specimen.

Figure 6 presents the crack formation and damage evolution in the tested specimens at the increasing load levels. At the first stage of the fracture process, two vertical cracks started to develop at the top and the bottom of the specimen. These cracks were initiated at $t = 960$ s ($n = 65$, $u = 0.54u_{\max}$) for specimen no. 1, at $t = 1005$ s ($n = 68$, $u = 0.63u_{\max}$) for specimen no. 2 and at $t = 1065$ s ($n = 72$, $u = 0.62u_{\max}$) for specimen no. 3 (the first column of photographs in Fig. 6). Next the horizontal splitting of the concrete prism appeared at $t = 1110$ s ($n = 75$, $u = 0.62u_{\max}$) for specimen no. 1, at $t = 1275$ s ($n = 86$, $u = 0.80u_{\max}$) for specimen no. 2 and at $t = 1245$ s ($n = 84$, $u = 0.73u_{\max}$) for specimen no. 3. This stage of damage is illustrated by the second column of photographs in Fig. 6. The penultimate stage of damage is given in the third column in Fig. 6. It occurred at $t = 1755$ s ($n = 118$, $u = 0.99u_{\max}$) for specimen no. 1, at $t = 1575$ s ($n = 106$, $u = 0.99u_{\max}$) for specimen no. 2 and at $t = 1695$ s ($n = 114$, $u = 0.99u_{\max}$) for specimen no. 3. The tensile tests were stopped as a result of the tension failure of the steel bar. Figure 7 shows the details of the concrete specimen after the splitting failure. The prints of the lugs of the reinforcing bar are clearly seen on the piece of damaged concrete. Therefore, the slipping of the steel bar and damage of the bar surrounding concrete by the tips of the rebar lugs did not take place.

3.2 Time and Frequency Representation of Ultrasonic Data

The interpretation of measured signals in the frequency domain was performed by the power spectral density (PSD). The PSD function was used since it shows the signal power that better displays the changes in the wave propagation signals due to material degradation than Fourier transform. The PSD was computed using MATLAB®. The examples of the ultrasonic signals acquired at point B for specimen no. 1 and their power spectral densities are shown in Fig. 8. It can be seen that at the initial stage, no significant differences were visible in the measured time signals (e.g. $n = 1$ and $n = 40$).

MOST WIEDZY Downloaded from mostwiedzy.pl

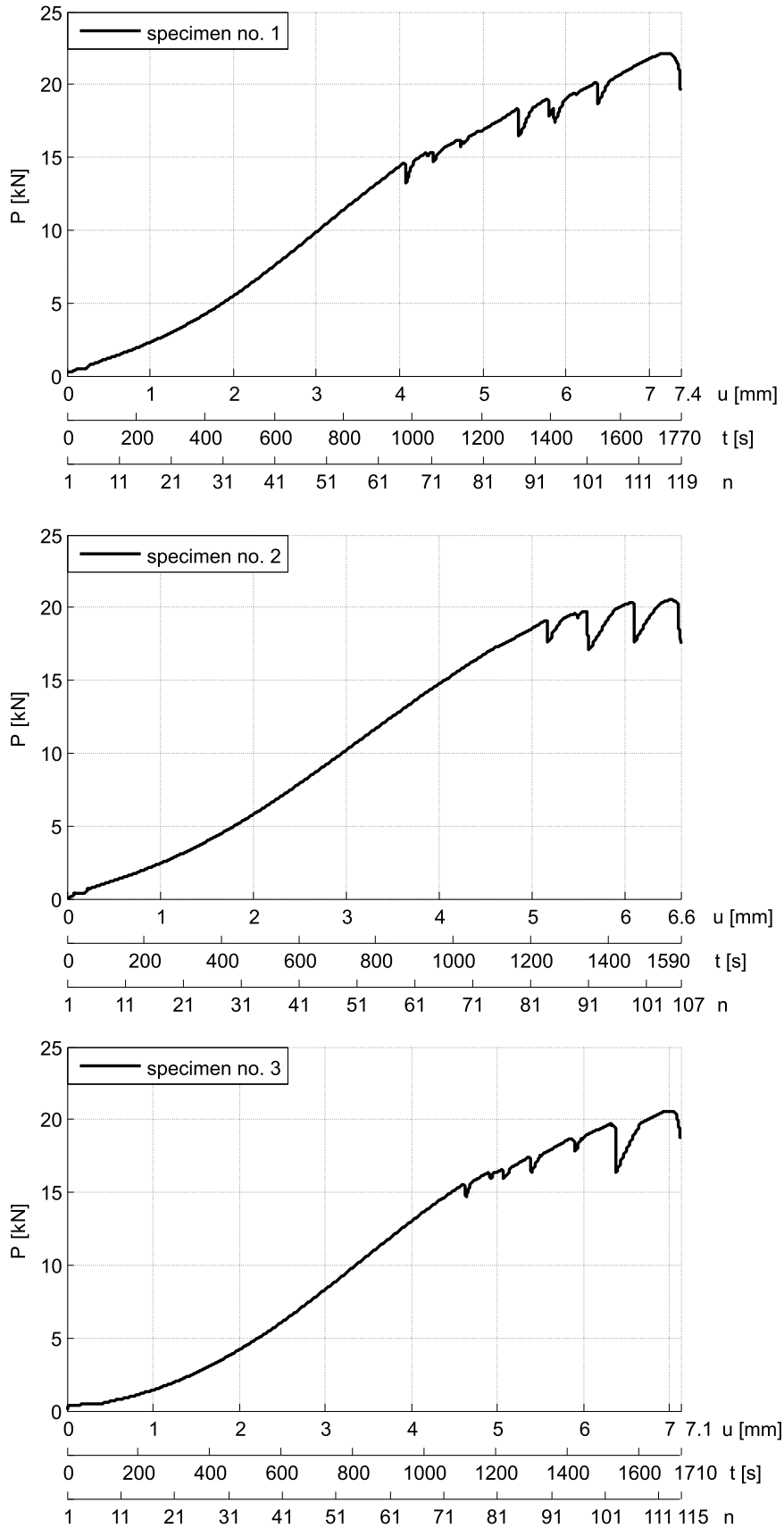

Fig. 5 Experimental load-deflection (P–u) and load-time (P–t) curves of three reinforced concrete specimens

MOST WIEDZY Downloaded from mostwiedzy.pl

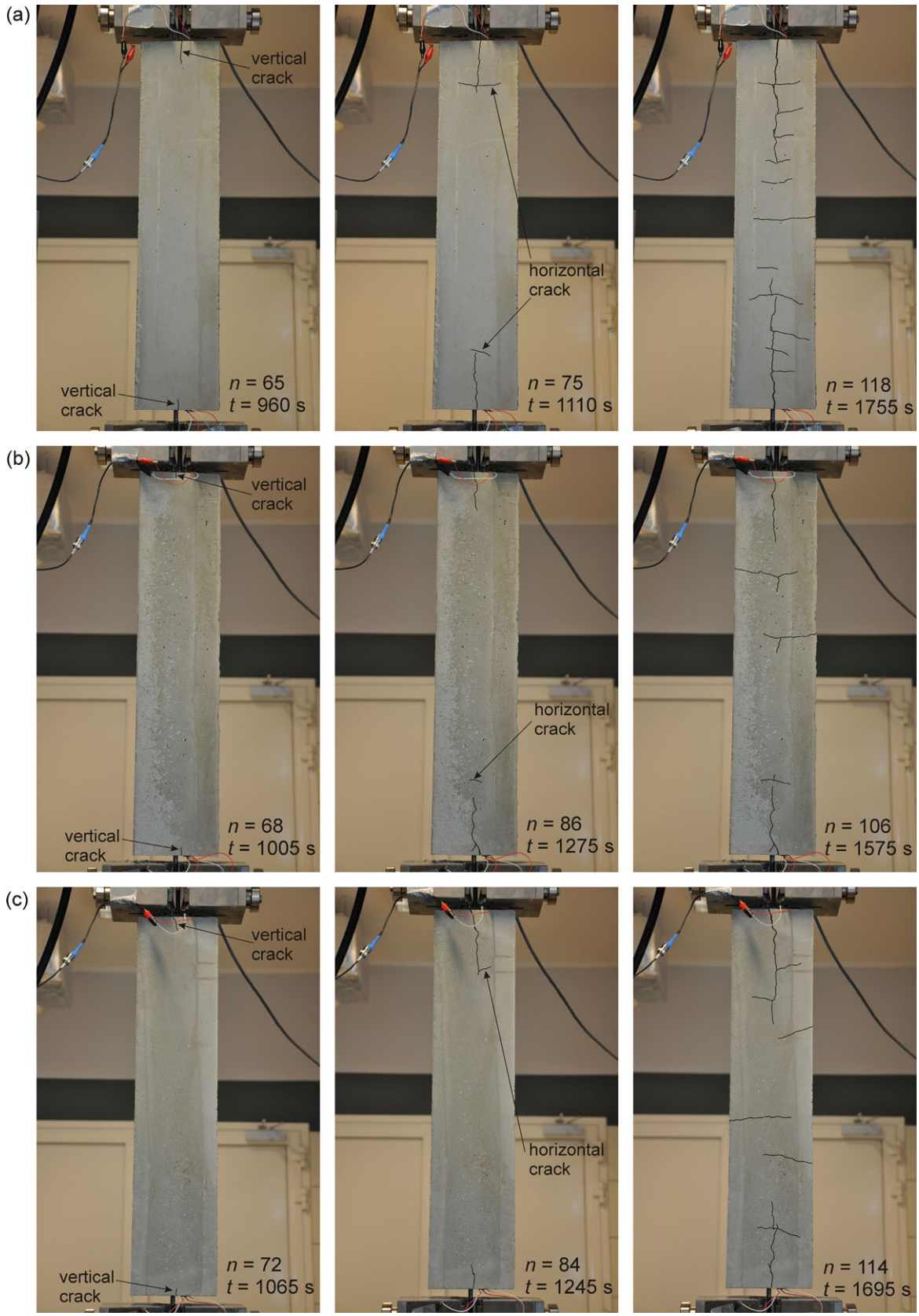

Fig. 6 Experimental damage evolution and crack patterns of three tested specimens (state of initiation of vertical cracks, state of initiation of horizontal cracks, penultimate stage of damage): (**a**) specimen no. 1; (**b**) specimen no. 2; (**c**) specimen no. 3

MOST WIEDZY Downloaded from mostwiedzy.pl

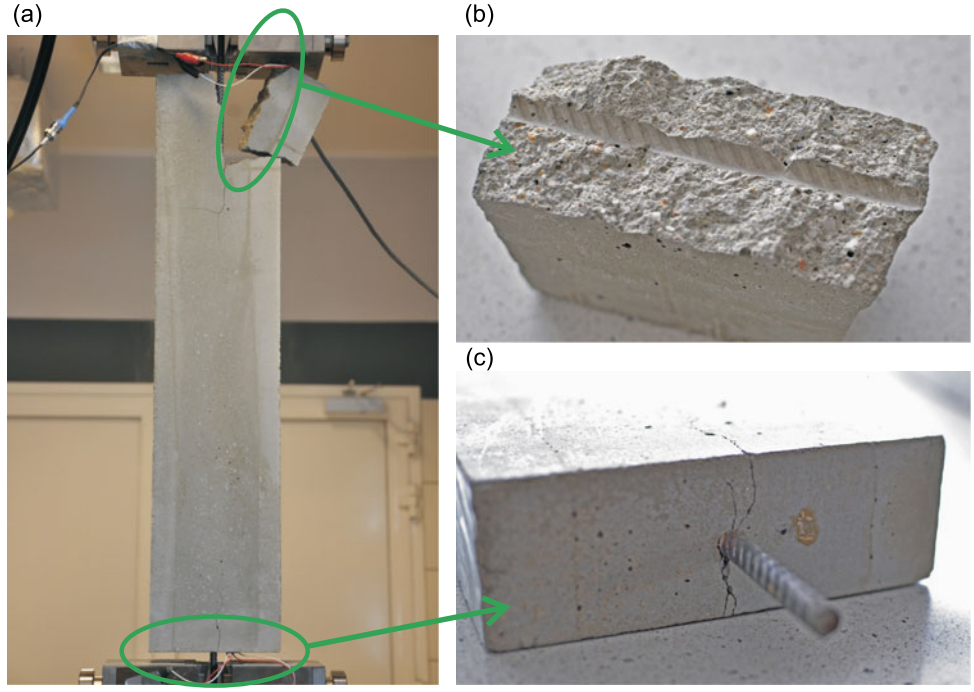

Fig. 7 Specimen no. 3 after damage: (**a**) the view of the specimen; (**b**) interface between steel and concrete; (**c**) splitting cracks on the bottom part of the specimen

The maximum amplitudes of the signals acquired at point B (on the opposite side then the PZT actuator) were practically the same for the signals from $n = 1$ to $n = 65$ and, then they decreased with the increase of the external tensile loading.

Figure 9 shows the peak values of the signals registered at point B for the specimen no. 1. Data in Fig. 9 are taken from the time signals (so called A-scans) for consecutive measurements of propagating ultrasonic waves. Peak values of the first incoming wave packet for the signals form $n = 1$ to $n = 119$ were plotted with white dots (Fig. 9). The first wave packet corresponds to the first pressure wave traveling in the specimen. The initial value of the peak was of about 80 mV. The first wave packet can be clearly seen for signal numbers from $n = 1$ to $n = 40$ (Fig. 9a). For the time records corresponding to higher signal numbers, the peak values of the first wave packet were determined for the time range $t = 0.27$–0.28 ms. The peak values of the second wave packet that can be seen at $t = 0.37$–0.38 ms were plotted in Fig. 9 with grey dots. The initial peak value of the second waveform was of about 200 mV. The second wave packet was associated with interference of shearing and pressure waves reflected from the specimen cross-section boundaries. The recognition which wave packet in the registered signal corresponds to pressure and shear waves was done based on wave velocities.

The amplitudes of the first wave packet were similar for the signal numbers from $n = 1$ to $n = 55$ (Fig. 9). From $n = 56$ to $n = 67$ the amplitudes started to decrease and from $n = 68$ they became close to zero. Small micro-cracked zones did not significantly affect the first pressure wave, and therefore, the significant drop of the maximum amplitudes was noticed when the first vertical crack appeared (at $n = 65$). The amplitudes of the second wave packet were constant for signal numbers from $n = 1$ to $n = 51$ and the relatively rapid decrease of the amplitudes took place till $n = 61$. At signal number $n = 75$ the maximum amplitudes of the second wave packet became very small. It seems that the change of the peak values of the second wave packet indicated the development of the micro-crack zone before splitting takes place. The vertical splitting cracks were observed for $n = 65$ while the reduction of the amplitudes starts at $n = 51$. Formations of micro-crack zones had relatively large influence on the reflected shear and pressure waves resulting in large attenuation of the second wave packet.

The evolution of the frequency spectrums in time for specimen no. 1, 2 and 3 are shown in Fig. 10. The power spectral densities of all ultrasonic signals acquired during the tensile test were plotted in the form of maps. White arrows indicate two characteristic measurements for each specimen: the measurement associated with the appearance of the first vertical crack and the measurement associated with the appearance of the first horizontal crack. The right column of Fig. 10 illustrates the power spectral densities of the A-scan signals measured at point B. It can be observed, that the amplitudes decreased with the increase of the damage stage. At the moment of the first vertical crack development, the amplitudes of the PSD revealed sudden change. The decrease in amplitudes occurred in a quasi-

MOST WIEDZY Downloaded from mostwiedzy.pl

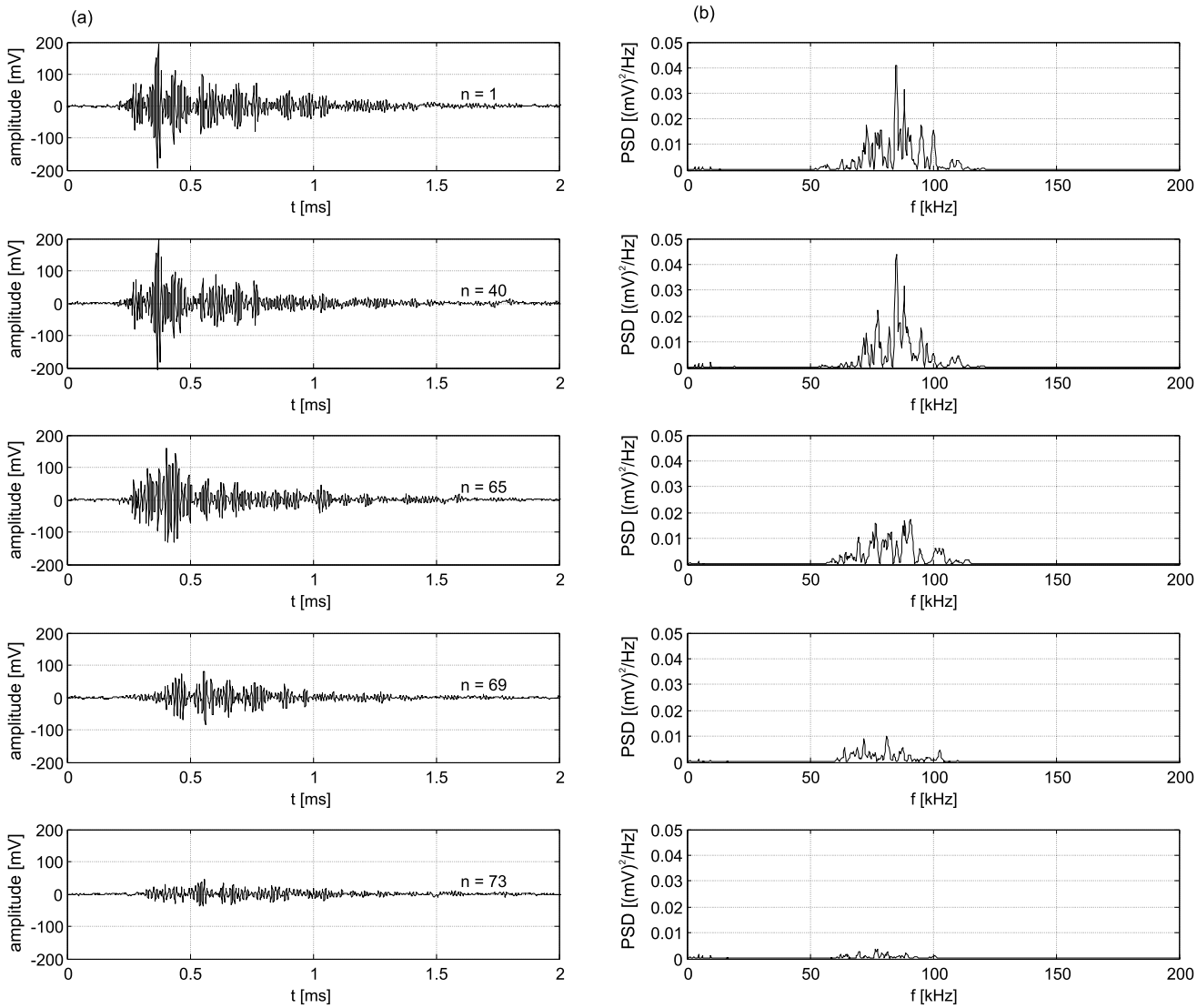

Fig. 8 Ultrasonic signals registered at point B in specimen no. 1 for different load levels: (**a**) A-scan signals in time domain; (**b**) power spectral densities of time waveforms

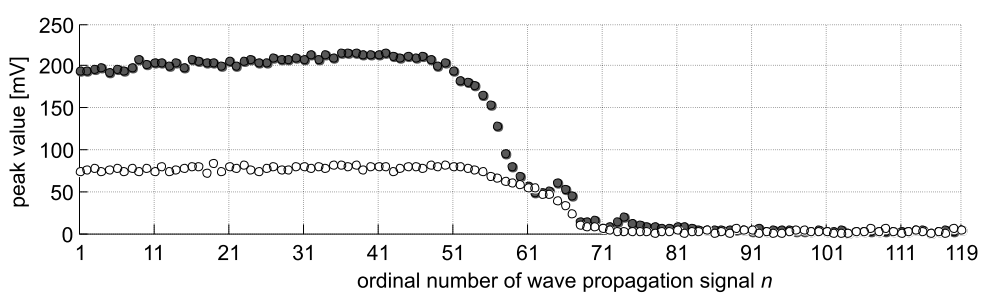

Fig. 9 Peak values of wave propagation signals registered at point B in the specimen no. 1: the first wave packet corresponding to the first pressure wave traveling in the specimen (*white dots*) and the second wave packet associated with interference of shearing and pressure waves reflected from the specimen cross-section boundaries (*grey dots*)

linear way, i.e. first higher frequency components decreased, while lower frequencies decreased at a later stage of damage.

The left column of Fig. 10 presents the power spectral densities of the signals measured at point A. These signals had similar amplitudes during all measurements because of

MOST WIEDZY Downloaded from mostwiedzy.pl

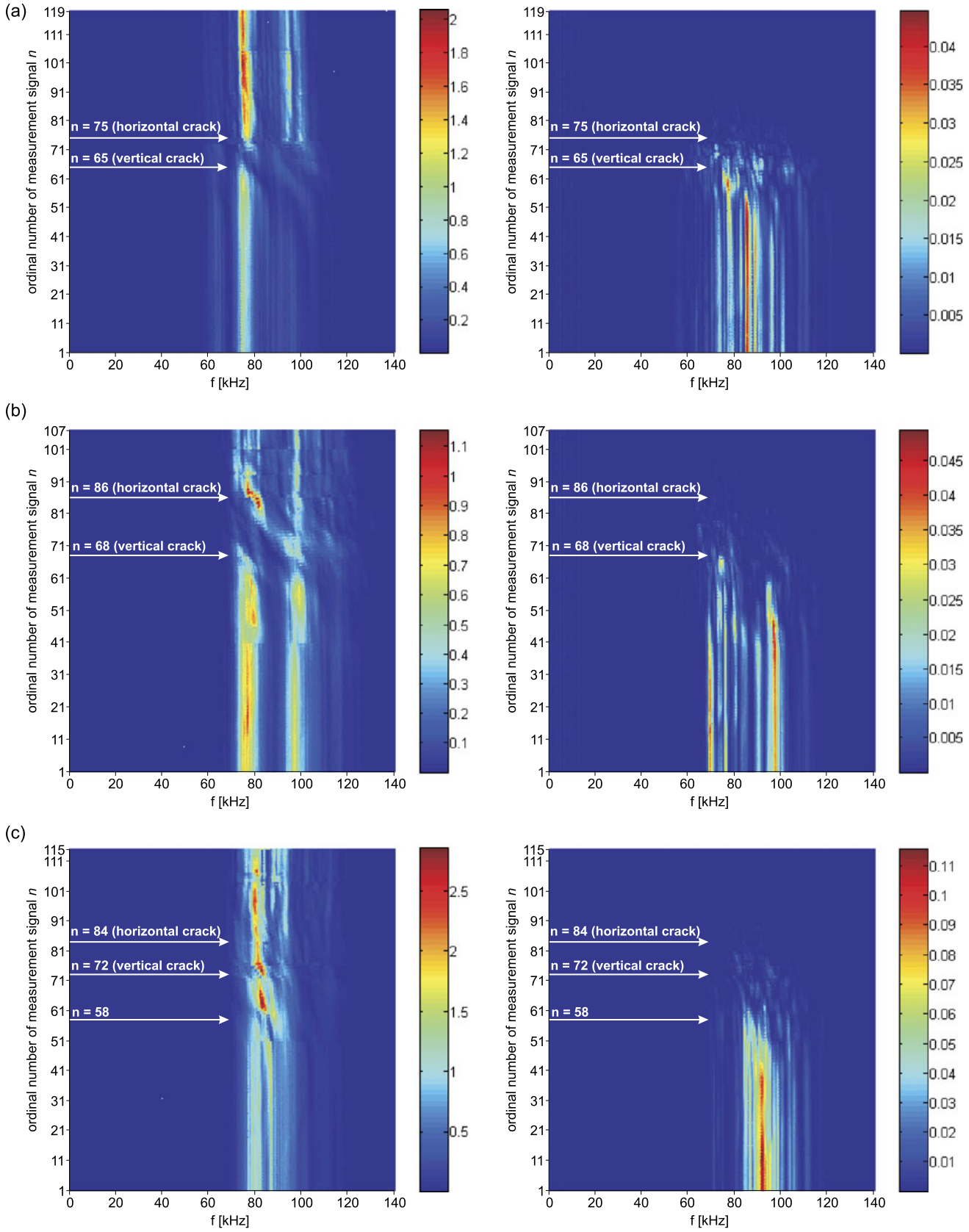

Fig. 10 Power spectral density maps of registered signals at point A (*left column*) and at point B (*right column*): (**a**) specimen no. 1; (**b**) specimen no. 2; (**c**) specimen no. 3 (power spectral densities are in units of $(mV)^2/Hz$)

MOST WIEDZY Downloaded from mostwiedzy.pl

their close location to the PZT actuator. Clear oblique lines are visible in the PSD maps for all specimens. At the moment of initiation of vertical crack, local decrease in the PSD amplitudes can be observed. It started at $n = 65$ for the specimen no. 1 and $n = 68$ for the specimen no. 2. This local decrease had an oblique line shape, i.e. first higher frequencies are damped, while the lower frequencies are damped at the next time instances. In the specimen no. 3 the first vertical crack was observed for measurement $n = 72$. However, it can be seen at the PSD map, that additional local decrease of amplitudes occurred ($n = 58$), probably as a result of other vertical crack on the opposite side (not monitored by camera).

3.3 Representation of Ultrasonic Data by Continuous Wavelet Transform

Details of the wave propagation in deteriorating concrete can be traced by the wavelet analysis. Selected ultrasonic signals were transformed by a continuous wavelet transform which gives a time-scale representation of the signal $x(t)$ [21]:

$$Wf(b,s) = \frac{1}{\sqrt{s}} \int_{-\infty}^{+\infty} x(t)\psi^*\left(\frac{t-b}{s}\right) dt, \tag{1}$$

where the variable t denotes time, $\psi(t)$ is a wavelet function and real numbers s and b denote the scale and translation parameters respectively. A time-scale representation of a signal is characterized by variable-sized regions. Wavelets allow using of short time intervals to obtain precise high frequency information and using longer time intervals for low frequency information. As the wavelet function $\psi(t)$, the complex Morlet function was used [22]:

$$\psi(t) = \frac{1}{\sqrt{\pi f_b}} e^{2i\pi f_c t} e^{-t^2/f_b}, \tag{2}$$

where f_b is a bandwidth parameter and f_c is a wavelet centre frequency. The applied parameters were $f_b = 4$ and $f_c = 4$.

The wavelet transform results for the selected A-scan signals for specimen no. 1 are presented in Fig. 11. The left column of Fig. 11 shows the wavelet coefficients of the signals registered at point A and the right column depicts the wavelet coefficients of signals registered at point B for time steps corresponding to $n = 55$ (stage before splitting), $n = 65$ (appearance of the first vertical splitting crack) and $n = 75$ (after the splitting failure). For $n = 55$, the elastic waves of frequency 76 kHz travelled through the concrete specimen and they can be observed in both signals measured at points A and B. At the beginning of development of the first splitting crack ($n = 65$), the micro-crack zones were the biggest, causing a significant reduction of the amplitudes of ultrasonic waves at points A and B. Wave packets had frequency range from 70 kHz to 100 kHz. Further increase of the external loading (e.g. $n = 75$) resulted in the appearance of several large splitting crack and yielding of the steel bar. Plastic deformation of the bar near the notch changed the longitudinal load distribution. Largest deformations were in the areas near the notches. The internal forces in the specimen in the region from its top (the location of point A) to the first horizontal splitting crack were reduced. Therefore, the micro-crack zone became smaller and the waves generated in the neighbourhood of the measurement point A could travel with relatively small damping. Figure 11a (left column) shows large wavelet coefficients at frequency 76 kHz and 96 kHz for the specimen after splitting failure ($n = 75$). The right column of Fig. 11b shows the wavelet coefficients of the signals at point B ($n = 75$). There are no large values of the wavelet coefficients since the specimen have been destroyed by the horizontal splitting cracks that prevented propagation of ultrasonic waves from point A to point B through the concrete.

4 Conclusions

In this paper the application of ultrasonic wave propagation method for inspection of reinforced concrete elements subjected to the splitting failure has been presented. A test procedure for health monitoring of damage evolution in reinforced concrete under increasing loading has been proposed. The proposed procedure is based on periodical excitation and acquisition of ultrasonic waves along the concrete prism by PZT transducers. The transducers are located on opposite sides of the concrete element subjected to tensile force. The analysis of the signals in time and frequency domain as well as by the wavelet transforms is a base for damage detection algorithm. The following concluding remarks can be drawn from the experimental study:

- The decrease of peak values of time signals registered at the end point has appeared at the moment of initiation of the first vertical cracks.
- The sudden decrease of amplitudes of the second wave packet could be observed before the appearance of the first vertical cracks was observed.
- Power spectral density amplitudes of signals from the points near the actuator and on the opposite side of the specimen clearly show the development of micro-crack zones and splitting failure. The initial stage of damage has been observed as a sudden decrease of the frequency spectra of the ultrasonic signals measured at the end point. For the signals acquired at the start point, a local decrease in the PSD amplitudes has appeared at the time, when the vertical cracks were initiated. The decrease in the PSD amplitudes has occurred in a quasi-linear way, i.e. first higher frequency components decreased, while lower frequencies decreased at a later stage of damage.

MOST WIEDZY Downloaded from mostwiedzy.pl

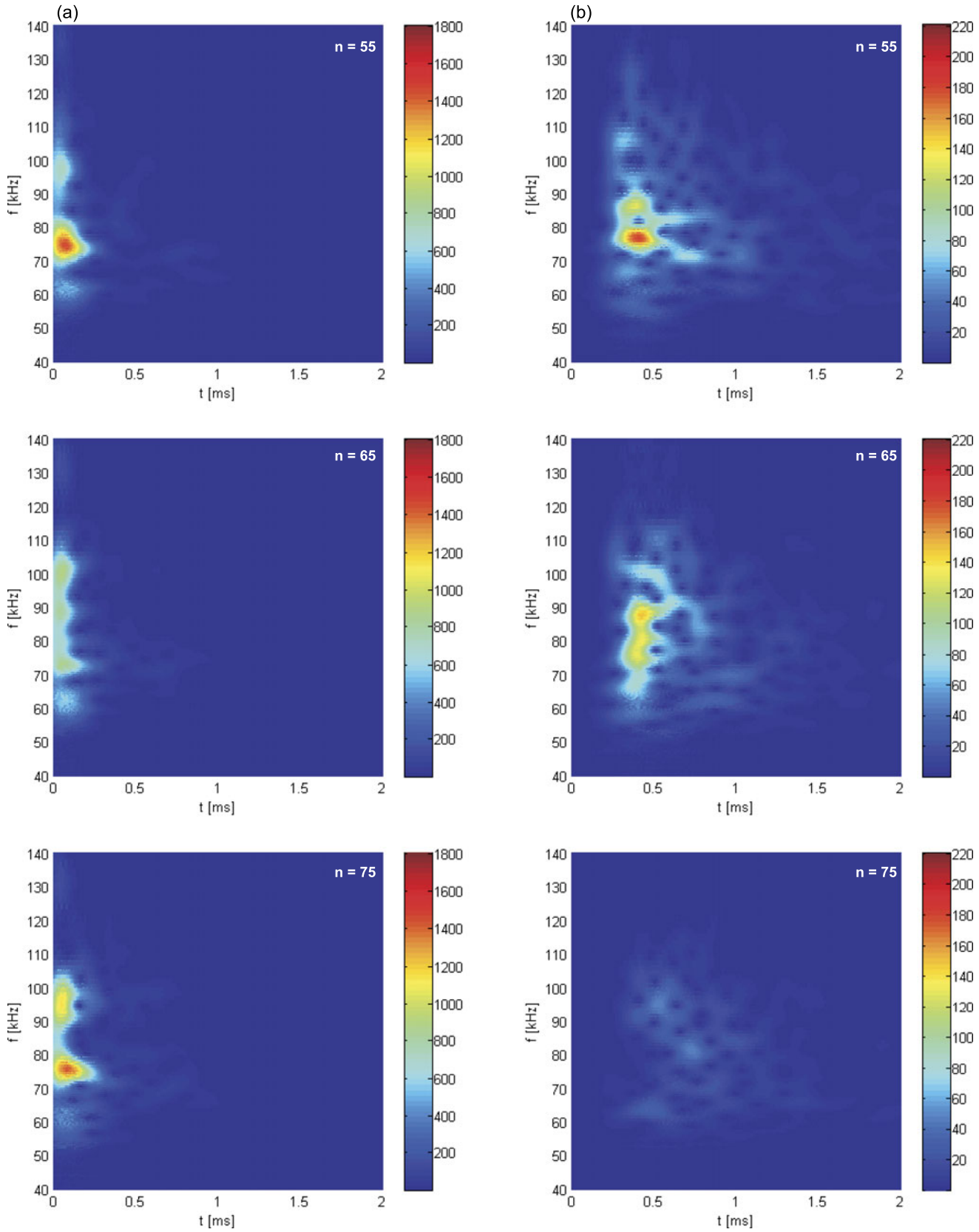

Fig. 11 Wavelet transforms for specimen no. 1 for different load levels: (**a**) signals registered at point A; (**b**) signals registered at point B (wavelet transforms are in units of mV)

MOST WIEDZY Downloaded from mostwiedzy.pl

- Application of the wavelet transforms allows focusing on cracking and allows precise detection of the splitting moment.
- The proposed testing procedure has enabled on-line health monitoring and identification of damage evolution in the reinforced concrete specimen subjected to tensile loading. The method has a potential to indicate the so called near failure stage, i.e., stage just before the splitting takes place.

The experimental studies presented in the paper were aimed at verification how micro-cracks zones affect the propagation of ultrasonic elastic waves in concrete before and after cracking. For the tested specimens PZT sensor A enabled detection of the appearance of the micro-cracking zone and PZT sensor B enabled detection of splitting failure. The proposed method tested on three specimens showed the possibility of detection of the moment before the appearance of cracks since it can detect the creation of micro-crack zones. However, the method appeared to be not suitable for detection of changes of size of crack zones in the tested specimens. Further studies on ultrasonic monitoring should focus on more realistic concrete elements like beams, plates or precast prestressed concrete elements of size used in construction as well as more realistic external loadings including combination of bending moments and normal forces. The studies should take into account the limitation on PZT transducers location in real concrete civil structures.

Acknowledgements This work reported in this paper has been supported by the project POIG 01.01.02-10-106/09 "Innovative means and effective methods to improve the safety and durability of building structures and transportation infrastructures in the strategy of sustainable development" within the Operational Programme Innovative Economy 2007–2013 co-financed from EU resources.

Open Access This article is distributed under the terms of the Creative Commons Attribution License which permits any use, distribution, and reproduction in any medium, provided the original author(s) and the source are credited.

References

1. Ohno, K., Ohtsu, M.: Crack classification in concrete based on acoustic emission. Constr. Build. Mater. **24**, 2339–2346 (2010)
2. Yun, H.-D., Choi, W.-C., Seo, S.-Y.: Acoustic emission activities and damage evaluation of reinforced concrete beams strengthened with CFRP sheets. Nondestruct. Test. Eval. Int. **43**, 615–628 (2010)
3. Clark, M.R., McCann, D.M., Forde, M.C.: Application of infrared thermography to the non-destructive testing of concrete and masonry bridges. Nondestruct. Test. Eval. Int. **36**, 265–275 (2003)
4. Iyer, S., Sinha, S.K., Pedrick, M.K., Tittmann, B.R.: Evaluation of ultrasonic inspection and imaging systems for concrete pipes. Autom. Constr. **22**, 149–164 (2012)
5. Molero, M., Aparicio, S., Al-Assadi, G., Casati, M.J., Hernández, M.G., Anaya, J.J.: Evaluation of freeze–thaw damage in concrete by ultrasonic imaging. Nondestruct. Test. Eval. Int. **52**, 86–94 (2012)
6. Krause, M., Milmann, B., Mielentz, F., Streicher, D., Redmer, B., Mayer, K., Langenberg, K.-J., Schickert, M.: Ultrasonic imaging methods for investigation of post-tensioned concrete structures: a study of interfaces at artificial grouting faults and its verification. J. Nondestruct. Eval. **27**, 67–82 (2008)
7. Algernon, D., Gräfe, B., Mielentz, F., Köhler, B., Schubert, F.: Imaging of the elastic wave propagation in concrete using scanning techniques: application for impact-echo and ultrasonic echo methods. J. Nondestruct. Eval. **27**, 83–97 (2008)
8. Schubert, F., Köhler, B.: Ten lectures on impact-echo. J. Nondestruct. Eval. **27**, 5–21 (2008)
9. Hoła, J., Sadowski, Ł., Schabowicz, K.: Nondestructive identification of delaminations in concrete floor toppings with acoustic methods. Autom. Constr. **20**, 799–807 (2011)
10. Yang, Y., Cascante, G., Polak, M.A.: Depth detection of surface-breathing crack in concrete plates using fundamental Lamb modes. Nondestruct. Test. Eval. Int. **42**, 501–512 (2009)
11. Tsai, Y.-T., Zhu, J.: Simulation and experiments of airborne zero-group-velocity Lamb waves in concrete plate. J. Nondestruct. Eval. **31**, 373–382 (2012)
12. Lammering, R.: Observation of piezoelectrically induced Lamb wave propagation in thin plates by use of speckle interferometry. Exp. Mech. **50**, 377–387 (2010)
13. Rucka, M.: Modelling of in-plane wave propagation in a plate using spectral element method and Kane-Mindlin theory with application to damage detection. Arch. Appl. Mech. **81**, 1877–1888 (2011)
14. Staszewski, W.J., Lee, B.C., Traynor, R.: Fatigue crack detection in metallic structures with Lamb waves and 3D laser vibrometry. Smart Mater. Struct. **18**, 727–739 (2007)
15. Mallet, L., Lee, B.C., Staszewski, W.J., Scarpa, F.: Structural health monitoring using scanning laser vibrometry: II: Lamb waves for damage detection. Smart Mater. Struct. **13**, 261–269 (2004)
16. Alleyne, D.N., Cawley, P.: The interaction of Lamb waves with defects. IEEE Trans. Ultrason. Ferroelectr. Freq. Control **39**, 381–397 (1992)
17. Giurgiutiu, V.: Structural Health Monitoring with Piezoelectric Wafer Active Sensors. Academic Press, Amsterdam (2008)
18. Gambarova, P.G., Rosati, G.P., Zasso, B.: Steel-to-concrete bond after concrete splitting: test results. Mater. Struct. **22**, 35–47 (1989)
19. Ogura, N., Bolander, J.E., Ichinose, T.: Analysis of bond splitting failure of deformed bars within structural concrete. Eng. Struct. **30**, 428–435 (2008)
20. Gálvez, J.C., Benítez, J.M., Tork, B., Casati, M.J., Cendón, D.A.: Splitting failure of precast prestressed concrete during the release of the prestressing force. Eng. Fail. Anal. **16**, 2618–2634 (2009)
21. Mallat, S.: A Wavelet Tour of Signal Processing. Academic Press, San Diego (1998)
22. Misiti, M., Misiti, Y., Oppenheim, G., Poggi, J.-M.: Wavelet toolbox. The MathWorks Inc. (2000)

MOST WIEDZY Downloaded from mostwiedzy.pl